The Vinyl Ether Linkages of Plasmalogens Are Favored Targets for Myeloperoxidase-Derived Oxidants: A Kinetic Study†

Ojia Skaff, David I. Pattison,* and Michael J. Davies

The Heart Research Institute, 114 Pyrmont Bridge Road, Camperdown, Sydney, NSW 2050, Australia

Received May 1, 2008; Revised Manuscript Received May 31, 2008

ABSTRACT: Plasmalogens, which contain a vinyl ether bond, are major phospholipids of the plasma membranes of endothelial and vascular smooth muscle cells and cardiac myocytes. These lipids, in contrast to other phospholipids, have been reported to be targets of HOCl/HOBr generated by myeloperoxidase, with elevated levels of the products of these reactions (α-chloro/α-bromo aldehydes and unsaturated lysophospholipids) having been detected in human atherosclerotic lesions. The reason(s) for the targeting of this lipid class, over other phospholipids, is poorly understood, and is examined here. It is shown that HOCl and HOBr react with a model vinyl ether (ethylene glycol vinyl ether) 200−300-fold faster (k = 1.6×10^3 and 3.5×10^6 M^{-1} s^{-1}, respectively) than with aliphatic alkenes (models of phospholipids). True plasmalogens react ca. 20-fold slower than the models. Chloramines and bromamines (from reaction of HOCl/HOBr with primary amines and α-amino groups) also react with vinyl ethers, unlike aliphatic alkenes, with $k = 10^{-3}-10^2$ M^{-1} s^{-1} for chloramines (with the His side chain chloramine being the most reactive, $k = 172$ M^{-1} s^{-1}) and $k = 10^3-10^4$ M^{-1} s^{-1} for bromamines. The bromamine rate constants are typically 10^5-10^6 larger than those of the chloramines. Intermolecular vinyl ether oxidation by phospholipid headgroup bromamines can also occur. These kinetic data indicate that plasmalogens are significantly more susceptible to oxidation than the aliphatic alkenes of phospholipids, thereby rationalizing the detection of products from the former, but not the latter, in human atherosclerotic lesions.

Myeloperoxidase (MPO[1]), a heme peroxidase released from the intracellular granules of many activated leukocytes, uses hydrogen peroxide (H_2O_2) to catalyze the production of hypohalous acids (HOX) from physiological concentrations of halides (Cl^-, Br^-, I^-) and pseudohalide (SCN^-) ions (reviewed *1, 2*). HOCl and HOBr are potent antibacterial agents crucial for the immune response; however, they can also induce deleterious reactions when generated at inappropriate levels, times and locations (*3*). These include the oxidation of heme groups, iron−sulfur centers, thiol and methionine residues and conversion of amine functions to chloramines and bromamines, which are reactive, potentially damaging, secondary oxidants (reviewed *1, 2*). Chloramines and bromamines, which can be formed on free amino acids, proteins, DNA, phospholipid headgroups and amino sugars, are less reactive and more selective oxidants than the parent HOX, and can readily diffuse into and within cells; as such they are likely to be critical intermediates in HOX-mediated damage (reviewed *1, 2, 4*). Previous studies have shown that bromamines are more reactive oxidants than the corresponding chloramines (*5, 6*), and that the pattern of reactivity of these species is somewhat different, with bromamines being less selective than chloramines (*6*).

Double bonds (alkenes) within the aliphatic chains of phospholipids are known to be targets for HOCl and HOBr (or reactive chlorinating and brominating species derived from these oxidants) released by activated phagocytes. These reactions, which occur at a slow rate relative to those of many protein components (reviewed (*6*)), yield chloro- and bromo-hydrins respectively (−CH═CH− → −CH(Cl/Br)−CH(OH)−), which disrupt membrane fluid molecular dynamics and may serve as markers of phagocyte-mediated inflammation (*7, 8*).

Plasmalogens constitute a subclass of glycerophospholipids found in the plasma membrane of mammalian endothelial and vascular smooth muscle cells and cardiac myocytes; in the human heart they account for ca. 30% of the total phospholipid content (*9*). Plasmalogens contain a vinyl ether bond linking the *sn*-1 aliphatic chain to the glycerol backbone, which has been reported to render them susceptible to oxidation compared with their 1-acyl analogues (*10*). HOX and halamine-derived products produced by MPO and activated neutrophils have been shown to attack the vinyl ether bond of plasmalogens. These reactions generate a different spectrum of products to those detected with other unsaturated phospholipids, with α-chloro- and α-bromo-

† This work was supported by grants from the Australian Research Council under the ARC Centres of Excellence program, and the National Health and Medical Research Council.

* To whom correspondence should be addressed. Telephone: +61-2-8208-8900. Fax: +61-2-9565-5584. E-mail: pattisond@hri.org.au.

[1] Abbreviations: 2-ClHDA, 2-chlorohexadecanal; HDL, high-density lipoproteins; HOBr, the physiological mixture of hypobromous acid and its anion; HOCl, the physiological mixture of hypochlorous acid and its anion; HOX, hypohalous acid; LDL, low-density lipoproteins; LPC, lysophosphatidylcholine; MPO, myeloperoxidase; NBr, bromamine; NCl, chloramine; $OOPC_{plasm}$, the plasmenyl-phospholipid, 1-*O*-1′-(*Z*)-octadecenyl-2-oleoyl-*sn*-glycero-3-phosphocholine; PC, phosphatidyl-choline; PE; phosphatidyl-ethanolamine; p-EA, phosphoryl-ethanolamine; POPC, 1-palmitoyl-2-oleoyl-*sn*-glycero-3-phosphocholine; PS, phosphatidyl-serine; p-Ser, phosphoryl-serine; Tau, 2-aminoethanesulfonic acid (taurine); TNB, 5-thio-2-nitrobenzoic acid; VE, vinyl ether.

10.1021/bi800786q CCC: $40.75
Published on Web 07/08/2008

aldehydes and unsaturated lysophospholipids reported as products (i.e., cleavage of the *sn*-1 linkage, in place of chlorohydrin formation); these materials appear to possess atherogenic properties (*11–13*). Although unsaturated phospholipids predominate over plasmalogens in vivo, chlorohydrins have not been detected at significant levels in advanced human atherosclerotic lesions, whereas it has been shown that α-chloro-aldehydes and unsaturated lysophospholipids are present at markedly elevated levels compared to normal aorta samples (*12*). This difference may be due to an enhanced rate of reaction of oxidants with plasmalogens over "normal" unsaturated phospholipids, despite the lower concentrations of plasmalogens, or that other factors (e.g., differing stability of the products, altered metabolism, differences in detection methods, and their corresponding limits of detection) are playing a role in modulating the levels of the various potential products measured in vivo. As plasmalogen degradation products are potential markers of inflammatory disease in tissues that contain this lipid class, such as the artery wall and the heart, it is important to understand which of these factors are key determinants in the formation and detection of these products. To date little is known about the kinetics of reactions of plasmalogens with hypohalous acids, and nothing is known, kinetically, about the potential reactions of chloramines and bromamines.

We have therefore examined the reaction kinetics of HOCl/HOBr, and a range of chloramines and bromamines, with vinyl ether-containing models of plasmalogens, and lipid plasmalogens themselves, by stopped-flow methods and competition kinetics. The occurrence of transfer reactions in plasmalogen models that contain both an amine group (as a site of initial chloramine formation) and a vinyl ether function has also been investigated.

EXPERIMENTAL PROCEDURES

Materials. The plasmenyl-phospholipid, 1-*O*-1′-(*Z*)-octadecenyl-2-oleoyl-*sn*-glycero-3-phosphocholine ($OOPC_{plasm}$), and the corresponding phospholipid, 1-palmitoyl-2-oleoyl-*sn*-glycero-3-phosphocholine (POPC), were obtained from Avanti Polar Lipids (Alabaster, MA, U.S.A.). Sodium hypochlorite in 0.1 M NaOH (low in bromide; BDH chemicals) was standardized by measuring A_{292nm} at pH 12 [ε_{292} ($^-$OCl) = 350 M^{-1} cm^{-1}] (*14*). All other chemicals were from Sigma/Aldrich/Fluka, except NaBr (>99%; Merck), and used without further purification. Chelex-treated phosphate buffer solutions (pH 7.4, 0.1 M or 10 mM for stopped-flow and HPLC, respectively) were prepared using Milli Q water.

Preparation of HOBr and Chloramines/Bromamines. HOBr was prepared by mixing equal volumes of HOCl (80 mM in H_2O, pH 13) and NaBr (90 mM in H_2O), followed by dilution (after 1 min) with 0.1 M phosphate buffer (pH 7.4) to the desired concentration (typically 0.03−1.0 mM). Fresh solutions were used for each kinetic run as HOBr disproportionates slowly to Br^- and BrO_2^- (*5, 15*). Chloramines and bromamines were prepared by mixing equal volumes of HOCl/HOBr (1 mM) with amine (50 mM), except for 4-imidazoleacetic acid chloramines where a 1.1-fold molar excess of substrate was used to maximize the stability of this material (*16, 17*). Fresh solutions were prepared for each kinetic run, and used within 30−60 min.

Quantification of Chloramines/Bromamines. 5-Thio-2-nitrobenzoic acid (TNB, 35−45 μM, prepared as described previously (*18*)), was used to assess chloramine/bromamine concentrations after incubation for 15 min using ε_{412} 14,150 M^{-1} cm^{-1} (*19*).

Stopped-Flow Studies. Stopped-flow studies were carried out using an Applied Photophysics SX.18MV system (0.01−10 s), or a Hi-Tech SFA 20 attachment to a PC-controlled Perkin-Elmer Lambda 40 UV/vis spectrometer (5−900 s) as described previously (*20, 21*). The oxidant was kept as the limiting reagent (typically 0.03−1 mM oxidant, 0.05−25 mM substrate), and kinetic data were analyzed by global methods using a multivariate data analysis program (Specfit32, version 3.0.37, Spectrum Software Associates) and confirmed by single wavelength analysis (OriginPro 7.0, OriginLab Corp. or Pro-Data Viewer 4.0, Applied Photophysics). All second-order rate constants were measured at 22 °C and pH 7.4, and are averages of at least four separate determinations, with errors specified as 95% confidence limits.

UV/Vis Spectroscopy. Spectra were recorded using a Perkin-Elmer Lambda 40 spectrometer, relative to a 0.1 M phosphate buffer baseline, between 220 and 320 nm (1−2 nm interval), with a time interval of 1−15 min depending on the reaction time scale. Temperature control (22 °C) was achieved with a Peltier block. Data were imported into Specfit software, and analyzed as described above.

HPLC Instrumentation and Methods. N-α-Acetyl-Tyr and its reaction products with HOCl and HOBr were separated and quantified using a gradient HPLC method as described previously (*21, 22*). Under the conditions employed, *N*-α-acetyl-Tyr, *N*-α-acetyl-Cl-Tyr, *N*-α-acetyl-Br-Tyr and *N*-α-acetyl-Br_2-Tyr eluted at ca. 13.1, 17.1, 18.8 and 30.7 min, respectively.

RESULTS

Reactions of Hypohalous Acids with Vinyl Ether Models of Plasmalogens. Stopped-flow analysis of the reaction of HOCl (1 mM) with the model compound ethylene glycol vinyl ether (5−20 mM, see Table 1 for structure) over 1 s showed a rapid decrease in absorbance over the range λ = 240−320 nm, with λ_{max} = 290 nm, consistent with $^-$OCl consumption (Figure 1a,b). The data were readily fitted, by global analysis methods, to a simple mechanism (HOCl + ethylene glycol vinyl ether → product) and yielded the second-order rate constant given in Table 1. Consistent results were obtained by fitting the data at 290 nm to a single-exponential function. The observed rate constants (k_{obs}) obtained from this fitting process were plotted against the substrate concentrations, with the gradient of the resulting straight line yielding an identical second-order rate constant (Figure 1c).

Reaction of HOBr with ethylene glycol vinyl ether was too fast to measure directly at 22 °C using stopped-flow methods, so a competition kinetics method using *N*-α-acetyl-Tyr as the reference substrate was employed (*21, 22*) with subsequent product quantification by HPLC. Reaction of HOBr (30 μM) with *N*-α-acetyl-Tyr (895 μM) was investigated in the absence and presence of increasing concentrations of ethylene glycol vinyl ether (0.05−1 mM). Addition of increasing vinyl ether concentrations inhibited the forma-

Table 1: Second-Order Rate Constants (with 95% Confidence Limits) at 22 °C and pH 7.4 in 0.1 M Phosphate Buffer (Except Where Otherwise Stated), for the Reactions of HOCl and HOBr with the Plasmalogen Model, Ethylene Glycol Vinyl Ether and the Lipid Plasmalogen, $OOPC_{plasm}$[A]

Substrate	Structure	k_2(HOCl) $M^{-1} s^{-1}$	k_2(HOBr) $M^{-1} s^{-1}$
Ethylene glycol vinyl ether	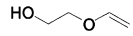	$(1.6 \pm 0.1) \times 10^3$ [a]	$(3.5 \pm 0.1) \times 10^6$ [b]
$OOPC_{plasm}$	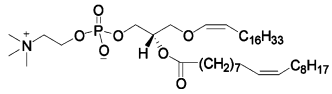	55 ± 7 [c]	N/A [d]

[A] Footnotes: [a] Determined by global analysis, an identical value was obtained by single wavelength analysis. [b] Determined by competition kinetics relative to *N*-α-acetyl-Tyr (10 mM phosphate buffer) using k(HOBr + *N*-α-acetyl-Tyr) = 2.6×10^5 M^{-1} s^{-1} (*22*), the calculated rate constant may be up to 30% higher due to systematic uncertainties (see text). [c] Determined by competition kinetics relative to *N*-α-acetyl-Tyr (10 mM phosphate buffer) using k(HOCl + *N*-α-acetyl-Tyr) = 47 M^{-1} s^{-1} (*23*). [d] Only an upper limit could be determined (see text).

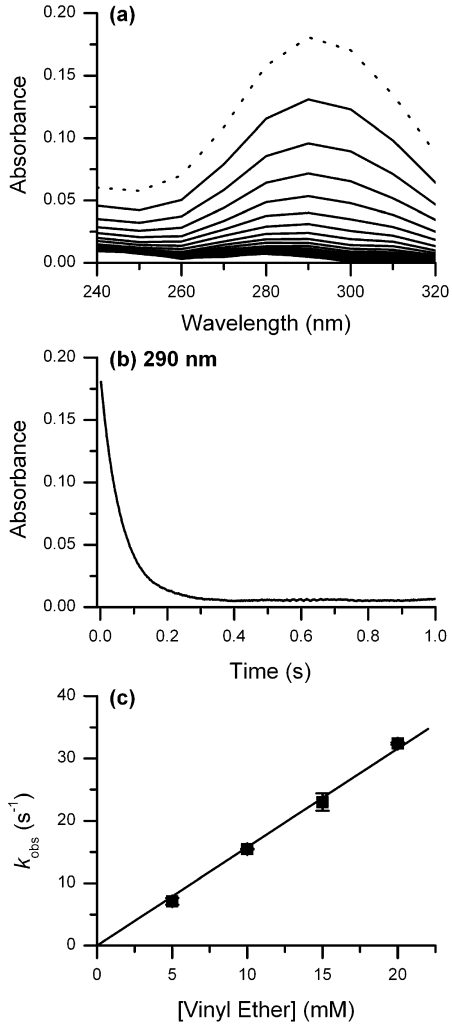

FIGURE 1: Kinetic data obtained for the reaction of ethylene glycol vinyl ether (10 mM) with HOCl (1 mM) at 22 °C and pH 7.4. (a) Time-dependent spectral data, with the dashed line at t = 2.5 ms and (b) a kinetic trace at 290 nm. (c) Plot of the observed rate constants (k_{obs}) versus substrate concentrations for HOCl (■), with k_{obs} determined by fitting the absorbance changes at 290 nm to a single-exponential decay. The fit was forced through the origin. Error bars represent standard deviations from repeated experiments. Some error bars are smaller than the size of the symbol.

tion of *N*-α-acetyl-Br-Tyr, and the resulting linear competition plots allowed the second-order rate constant to be

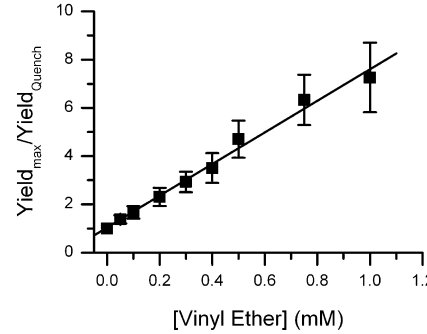

FIGURE 2: Plot of the linear analysis for the competitive kinetic data obtained by HPLC methods for the reaction of HOBr (30 μM) with *N*-α-acetyl-Tyr (895 μM) in the presence of increasing concentrations of ethylene glycol vinyl ether (0.05−1 mM) (■), determined from UV data. Error bars represent standard deviations from repeated experiments. Some error bars are smaller than the size of the symbol.

Scheme 1: Postulated Reactions and Mechanisms That Occur Following the Addition of HOX (X = Cl, Br) to Model Compound 2-Aminoethyl Vinyl Ether, Containing Both a Free Amine Group and a Vinyl Ether Bond

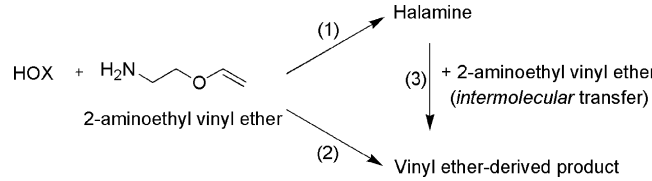

determined (Figure 2; Table 1) (*22*). As this method does not allow for the formation of *N*-α-acetyl-3,5-dibromotyrosine, a known product of *N*-α-acetyl-Tyr oxidation which complicates the analyses (*21, 22*), the actual rate constant may be up to 30% higher than given in Table 1.

As many plasmalogens also contain a free amine in the phospholipid headgroup (*9*), which is a potential competing target for reaction with HOX, the reactions of HOCl and HOBr with the model compound, 2-aminoethyl vinyl ether, were also examined (Scheme 1). The reaction kinetics for HOCl (0.1−0.25 mM) were monitored with substrate concentrations from 250 μM to 1.8 mM. Stopped-flow studies showed a rapid loss in absorbance at 290 nm (Figure 3a), consistent with $^-$OCl consumption. However, at lower wavelengths (<270 nm), rapid increases (25−200 ms) in absorbance were observed (Figure 3b), consistent with

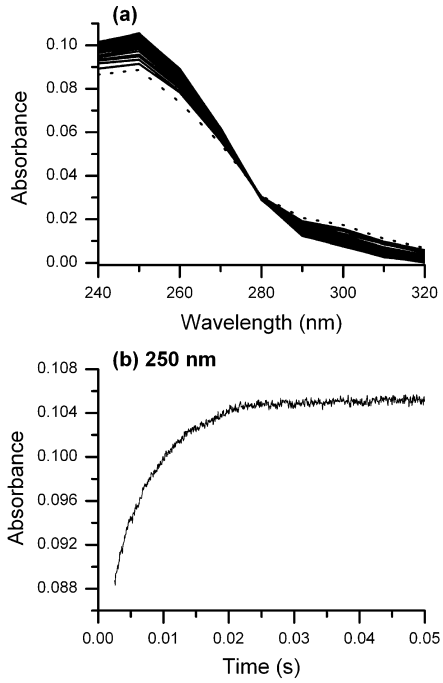

FIGURE 3: Kinetic data obtained for the reaction of 2-aminoethyl vinyl ether (0.8 mM) with HOCl (0.1 mM) at 22 °C and pH 7.4. (a) Time-dependent spectral data, with the dashed line at $t = 2.5$ ms, and (b) a kinetic trace obtained at 250 nm.

chloramine formation rather than vinyl ether oxidation. The isosbestic point at ca. 280 nm (Figure 3a) supports a simple reaction mechanism (HOCl + 2-aminoethyl vinyl ether → chloramine) (Scheme 1; reaction 1). Global analysis fitting of the kinetic data to this mechanism yielded a second-order rate constant of $(2.2 \pm 0.4) \times 10^5$ M^{-1} s^{-1} for chloramine formation; single wavelength analysis (250 nm) provided a consistent rate constant ($(2.1 \pm 0.1) \times 10^5$ M^{-1} s^{-1}). For the corresponding HOBr reaction, instantaneous increases in absorbance over the full spectral range were consistent with bromamine formation but were too fast to measure accurately by stopped-flow methods at 22 °C.

The potential occurrence of secondary chlorine transfer from the initially generated chloramine to the vinyl ether group was investigated over a period of 18 h (Scheme 1; reaction 3). Over this extended time scale, no further absorbance changes were detected, suggesting that no chlorine transfer occurred. In contrast, examination of the reaction of HOBr (0.1 mM) with 2-aminoethyl vinyl ether (0.5−1.5 mM) over longer time scales (50−100 s) resulted in further absorbance changes, consistent with the occurrence of secondary reactions. The data were analyzed by global methods using the mechanism in Scheme 1, and yielded a second-order rate constant, for reaction 3 of 170 ± 30 M^{-1} s^{-1}; single wavelength analysis at 260 nm gave a similar value (150 ± 30 M^{-1} s^{-1}). The observed rate constants were dependent on the 2-aminoethyl vinyl ether concentration, consistent with *intermolecular* bromine transfer.

Reactions of Hypohalous Acids with Lipid Plasmalogens. To assess whether lipid plasmalogens react with similar rate constants to the model vinyl ethers, the reactions of HOCl/HOBr with the plasmenyl-phospholipid, $OOPC_{plasm}$, were investigated by competition kinetics (as above). The rate constant for reaction of $OOPC_{plasm}$ was obtained from experiments where HOCl (30 μM) was rapidly mixed with

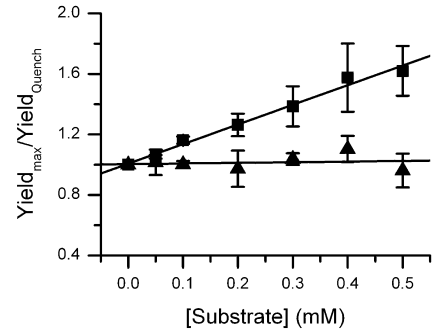

FIGURE 4: Plots of the data and linear analysis for the competitive kinetic data obtained by HPLC methods for the reaction of HOCl (30 μM) with *N*-α-acetyl-Tyr (895 μM) in the presence of increasing concentrations of POPC (▲) and $OOPC_{plasm}$ (■) (0.05−0.5 mM), determined from UV data. Error bars represent standard deviations from repeated experiments. Some error bars are smaller than the size of the symbol.

$OOPC_{plasm}$ (0.05−0.5 mM) in the presence of *N*-α-acetyl-Tyr (895 μM), and the yield of halogenated *N*-α-acetyl-Tyr quantified by HPLC. *N*-α-Acetyl-Cl-Tyr formation was inhibited by increasing concentrations of $OOPC_{plasm}$; analysis of the competition kinetic data provided the second-order rate constant (Figure 4; Table 1) (*22, 23*). Experiments using the analogous non-plasmenyl phospholipid POPC (0.05−1 mM) did not show any inhibition of *N*-α-acetyl-Cl-Tyr formation (Figure 4). These data provide an upper limit for the rate constant for reaction of HOCl with POPC of 5 M^{-1} s^{-1}.

Analogous experiments to those outlined above were carried out with HOBr. Reaction of this oxidant (30 μM) with $OOPC_{plasm}$ (0.025−0.5 mM) did not result in any inhibition of *N*-α-acetyl-Br-Tyr formation, thus only an upper limit for the rate constant could be obtained, $k < 5 \times 10^4$ M^{-1} s^{-1}. Similarly, with POPC and HOBr an upper limit rate constant was obtained of $k < 3 \times 10^4$ M^{-1} s^{-1}. It should be noted that, based on previous data for the reactions of HOBr with double bonds (*21*), and the suppression in reactivity observed for HOCl with $OOPC_{plasm}$ vs ethylene glycol vinyl ether, the actual rate constants are likely to be significantly lower than these limits. Overall, however, these data for both HOCl and HOBr indicate that the plasmalogen is considerably more reactive than the non-vinyl ether-containing substrate.

Reactions of Isolated Phospholipid Headgroup-Derived Chloramines and Bromamines with Plasmalogen Model Compounds. The reactivity of ethylene glycol vinyl ether with chloramines/bromamines generated on phosphoryl-serine (p-Ser) and phosphoryl-ethanolamine (p-EA) were examined. The UV/vis absorbance changes observed on reaction of p-Ser chloramine (1 mM) with ethylene glycol vinyl ether (5−20 mM) across the wavelength range 240−320 nm obeyed simple pseudo-first-order kinetics (chloramine + ethylene glycol vinyl ether → product) to yield a second-order rate constant (Table 2). Analysis of the corresponding p-Ser bromamine reaction was more complex due to the unstable nature of this bromamine (TNB assays indicate that this compound decays in <10 min), thereby preventing accurate determination of the second-order rate constant; however, an estimate of ca. 2.7×10^4 M^{-1} s^{-1} was obtained.

Table 2: Second-Order Rate Constants (with 95% Confidence Limits) Obtained by Global Analysis at 22 °C and pH 7.4 (in 0.1 M Phosphate Buffer) for the Reactions of Various Biologically-Relevant Halamines with the Plasmalogen Model, Ethylene Glycol Vinyl Ether

Halamine	k_2(NCl),[a] M^{-1} s^{-1}	k_2(NBr),[b] M^{-1} s^{-1}
	Lipid Headgroups	
Phosphoryl-ethanolamine	$(1.2 \pm 0.1) \times 10^{-2}$	$(1.5 \pm 0.1) \times 10^{4}$
Phosphoryl-serine	$(4.3 \pm 1.6) \times 10^{-2}$	N/A[c]
	Protein Amine Groups	
N-α-Acetyl-Lys	$(1.1 \pm 0.2) \times 10^{-2}$	$(4.0 \pm 0.1) \times 10^{3}$
4-Imidazoleacetic acid	104 ± 12	N/A[d]
	Free Amino Acids	
Taurine	$(5.1 \pm 0.4) \times 10^{-3}$	$(1.31 \pm 0.03) \times 10^{3}$

[a] The chloramine rate constants (M^{-1} s^{-1}) obtained by global analysis were confirmed by single wavelength analysis; k(p-EA) = $(1.1 \pm 0.1) \times 10^{-2}$; k(p-Ser) = $(3.7 \pm 0.8) \times 10^{-2}$; k(*N*-α-Acetyl-Lys) = $(1.1 \pm 0.2) \times 10^{-2}$; k(4-imidazoleacetic acid) = 120 ± 40; k(Tau) = $(5.5 \pm 1.2) \times 10^{-3}$. [b] The bromamine rate constants (M^{-1} s^{-1}) obtained by global analysis were confirmed by single wavelength analysis; k(p-EA) = $(1.38 \pm 0.04) \times 10^{4}$; k(*N*-α-Acetyl-Lys) = $(3.8 \pm 0.3) \times 10^{3}$; k(Tau) = $(1.3 \pm 0.1) \times 10^{3}$. [c] Approximate determination by single wavelength analysis yielded $k \sim 2.7 \times 10^{4}$ M^{-1} s^{-1}. [d] Unable to measure kinetics due to bromamine instability.

Corresponding studies of the reaction of p-EA-derived chloramine (1 mM) with ethylene glycol vinyl ether (10−25 mM) over 12.5−18 h showed a decrease in absorbance from λ 235 to 300 nm due to chloramine consumption. Data analysis using a simple mechanism (chloramine + ethylene glycol vinyl ether → product) gave the second-order rate constant (Table 2). The related p-EA bromamine (0.25 mM) was also investigated with 1−10 mM ethylene glycol vinyl ether. A rapid initial decay, followed by a slower decrease in absorbance was observed at all monitored wavelengths (λ = 240−320 nm) over a time scale of 0.5−2 s. Maximal changes in absorbance were observed at 240 and 280 nm; analysis of the fast decay process yielded a rate constant that has been assigned to reaction of the bromamine with the vinyl ether bond (Table 2). The processes responsible for the secondary decay are unclear; this data could not be fitted satisfactorily by first-order or second-order mechanisms.

Reactions of Protein-Derived, and Other, Halamines with Plasmalogen Model Compounds. As amino acid side chains on proteins are important kinetic targets for HOCl (reviewed (*6*)), and can initiate secondary oxidation (*15, 24*), the reactions of these species with plasmalogen models were examined. Reaction of ethylene glycol vinyl ether (10−25 mM) with *N*-α-acetyl-Lys chloramine (1 mM) resulted in absorbance changes over 18 h across the wavelength range 240−320 nm consistent with chloramine consumption. Global analysis of the data using a simple mechanism (chloramine + ethylene glycol vinyl ether → product) yielded the second-order rate constant given in Table 2. Reaction of the corresponding bromamine (0.25 mM) was also investigated over a period of 0.25−2 s. The bromamine absorbance decayed over the full spectral range (λ = 240−320 nm) with pseudo-first-order kinetics and yielded a second-order rate constant (Figure 5a,b; Table 2), with consistent data obtained by single wavelength analysis (280 nm) (Figure 5c). As observed with p-EA bromamine and ethylene glycol vinyl ether, a secondary decay in absorbance occurred over longer time scales (50 s), but again the nature of this process could not be elucidated from the data available.

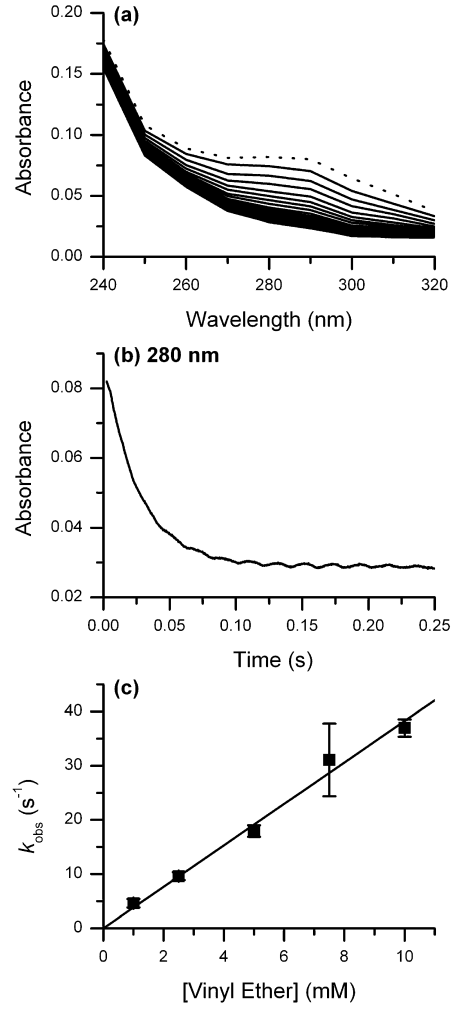

FIGURE 5: Kinetic data obtained for the reaction of *N*-α-acetyl-Lys bromamine (0.25 mM) with ethylene glycol vinyl ether (10 mM) at 22 °C and pH 7.4. (a) Time-dependent spectral data, with the dashed line at t = 2.5 ms, and (b) a kinetic trace at 280 nm. (c) Plot of the observed rate constants (k_{obs}) versus substrate concentrations for *N*-α-acetyl-Lys bromamine (■), with k_{obs} determined by fitting the absorbance changes at 280 nm to a single-exponential decay. The fit was forced through the origin. Error bars represent standard deviations from repeated experiments. Some error bars are smaller than the size of the symbol.

The reaction of the vinyl ether with the His side chain chloramine was investigated using the model compound, 4-imidazoleacetic acid chloramine (*16, 17*). The reaction of this species (0.5 mM) with ethylene glycol vinyl ether (2.5−15 mM) resulted in loss of the spectral features of the chloramine (λ = 240−320 nm, with λ_{max} = 240 nm) over 5−50 s, with this dependent on the vinyl ether concentration. Global analysis (chloramine + ethylene glycol vinyl ether → product) yielded the second-order rate constant given in Table 2. Analogous studies with the bromamine were not possible due to the instability of this species.

Reaction with taurine (Tau; 2-aminoethanesulfonic acid) chloramine resulted in the loss of the chloramine absorbance (λ_{max} = 250 nm) over a period of 18 h (Figure 6a,b). The data were analyzed, as above, to give the rate constant given in Table 2 and confirmed by single wavelength analysis (Figure 6c). The corresponding bromamine (0.25 mM) was consumed over 0.5−10 s on reaction with ethylene glycol vinyl ether (1−10 mM) and yielded the second-order rate

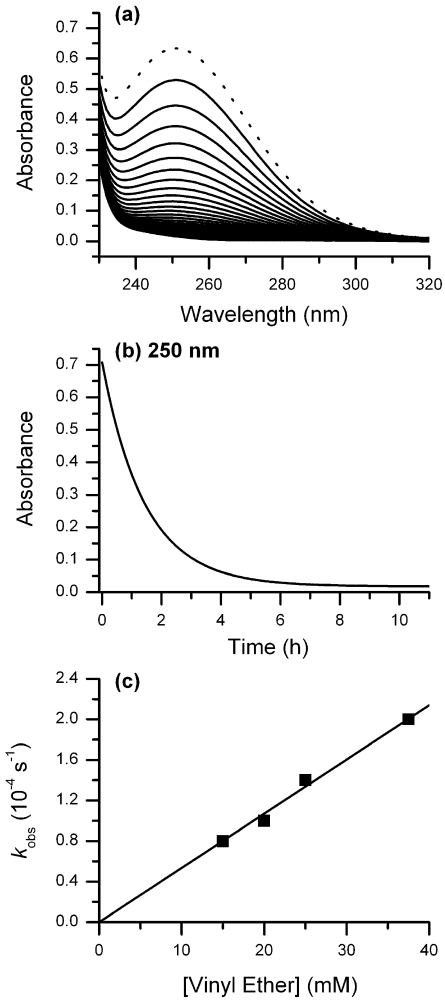

FIGURE 6: Kinetic data obtained for the reaction of taurine chloramine (2 mM) with ethylene glycol vinyl ether (37.5 mM) at 22 °C and pH 7.4. (a) Time-dependent spectral data, with the dashed line at $t = 15$ s, and (b) a kinetic trace at 250 nm. (c) Plot of the observed rate constants (k_{obs}) versus substrate concentrations for taurine chloramine (■), with k_{obs} determined by fitting the absorbance changes at 250 nm to a single-exponential decay. The fit was forced through the origin.

constant given in Table 2. Unlike the corresponding reactions of p-EA and *N*-α-acetyl-Lys bromamines, no subsequent changes in absorbance were observed over longer time scales.

DISCUSSION

Plasmalogen phospholipids, that contain a vinyl ether linkage at the *sn*-1 position, account for almost 20% of the phospholipid mass in humans (*9*). These lipids are typically phosphatidyl-ethanolamine (PE) and phosphatidyl-choline (PC) species. PE plasmalogens are found at high levels in the brain and spermatozoa (*9*), whereas the heart contains a higher proportion of PC plasmalogens (*9*). Plasmalogens comprise ca. 5% of the total phospholipid pool in plasma, with marginally more PC than PE species (*25*). Of the PE phospholipids found in plasma, around 55% are plasmalogens, whereas only ca. 5% of the PC phospholipids are plasmalogens (*26*); these ratios are similar for the low-density lipoprotein (LDL) and high-density lipoprotein (HDL) fractions of plasma (*26*). Interestingly, ca. 50−70% of the PE phospholipids in macrophages, monocytes and neutrophils are plasmalogens (*9*). The abundance of these species may therefore make them targets for MPO- and eosinophil peroxidase-derived oxidants, and particularly HOCl and HOBr.

It has been proposed that the vinyl ether bond makes plasmalogens more susceptible to oxidation than their 1-acyl analogues (*11*). It has also been suggested that plasmalogens may act as endogenous antioxidants that can scavenge reactive species such as peroxyl radicals, thereby protecting other phospholipids and lipoproteins from damage (*9*). Recent studies have demonstrated that plasmalogens are major phospholipid targets for HOCl, HOBr and chloramines/bromamines, and that the vinyl ether moieties are particularly susceptible to modification (*11–13, 27, 28*). The kinetic data reported here quantify this enhanced susceptibility for the first time.

HOCl reacts with the plasmalogen model, ethylene glycol vinyl ether, with a second-order rate constant ca. 180-fold greater than that of 3-pentenoic acid which has been used as a model for the unsaturated bonds of fatty acid side chains (*20*). The corresponding rate constant for HOBr is ca. 2000-fold greater than that for HOCl, and ca. 320 times greater than that for reaction with 3-pentenoic acid (*21*). This is consistent with the much higher reactivity of double bonds and aromatic amino acid residues (e.g., Tyr, Trp) with HOBr than HOCl (*6, 20–23*) and is due to the enhanced electrophilicity of HOBr compared with HOCl.

Although ethylene glycol vinyl ether is a useful model of a plasmalogen linkage and provides insight into the reactivity of vinyl ethers with HOCl and HOBr, phospholipids have more complex structures that may influence the rate of these reactions. Thus, $OOPC_{plasm}$ was also examined, and it has been shown that the rate constant for the reaction of this species with HOCl is >10-fold larger than that for the non-vinyl ether-containing substrate POPC; these data confirm that the vinyl ether linkage is highly susceptible to HOCl, and more so than a standard nonconjugated alkenic phospholipid. The rate constant for reaction of HOCl with $OOPC_{plasm}$ is ca. 30 times smaller than that for the model vinyl ether, consistent with previous reports that have shown a decrease in the rate constants for the reaction of HOX with unsaturated phospholipids (*29*) compared with isolated double bonds (Table 1) (*21*). This has been attributed to the formation of lipid structures, such as liposomes or micelles, where the double bond is buried in a hydrophobic environment, into which HOX is less permeable. However, it might be expected that this would affect plasmenyl linkages less than unsaturated *sn*-2 side chains, as the vinyl ether moiety is in close proximity to the polar amine headgroup, which is likely to be present at the interface with the aqueous phase. Whatever the reason for this depression of the rate constants from isolated vinyl ethers to $OOPC_{plasm}$ or POPC, it renders them unable to compete with the rapid bromination of *N*-α-acetyl-Tyr (*22*), thereby precluding accurate determination of the rate constants for HOBr with $OOPC_{plasm}$ or POPC.

The plasmalogen chosen for these studies contains a phosphatidyl-choline (PC) headgroup that reacts slowly with HOCl and HOBr (*20, 30*) thereby limiting reaction of HOX to the vinyl ether linkage or unsaturated fatty acid side chain. However, some phospholipids contain polar headgroups that contain amine functions with which HOCl/HOBr may also react (e.g., phosphatidyl-serine (PS) and phosphatidyl-ethanolamine (PE) species) (*20, 21, 31*). This is of particular

relevance for plasmalogens, as PE is the predominant headgroup, with the remainder being PC species (*9*). The potential role of such amine groups as an alternative site of initial reaction, and a possible source of chloramines/bromamines that could initiate secondary oxidation of the vinyl ether, was therefore investigated. The data obtained with 2-aminoethyl vinyl ether, a model of PE plasmalogens, indicates that HOCl reacts almost exclusively at the amine group to form the vinyl ether chloramine, despite the enhanced reactivity of the vinyl ether group compared with other alkenes; the resulting chloramine does not appear to initiate secondary oxidation of the vinyl ether bond (Scheme 1). HOBr also targets the amine group of 2-aminoethyl vinyl ether, but, in this case, the resulting bromamine was able to subsequently oxidize the vinyl ether bond via an *intermolecular* reaction. In the light of this positive data, the chloramines and bromamines formed on model lipid headgroups (p-EA and p-Ser) were also examined and are able to oxidize ethylene glycol vinyl ether. The second-order rate constants obtained for the oxidation of the vinyl ether by these chloramines are 10^4-10^5 times slower than the corresponding reactions of HOCl, whereas those for the bromamines are only 100−200 times slower than the HOBr reactions. These data contrast with that for non-plasmenyl unsaturated phospholipids where HOCl reacts almost exclusively with the PE headgroup in non-plasmenyl phospholipids (*31*), whereas HOBr reacts equally with the headgroup and the unsaturated fatty acid side chains (*31*).

In complex biological fluids such as plasma, protein-bound- and free amino acid-chloramines and bromamines are major intermediates in HOCl and HOBr reactions due to the abundance of these targets (Pattison et al., unpublished data) (*20, 21*). In neutrophils, the sulfonated amino acid Tau is highly abundant (concentrations ≤20 mM (*32*)) and therefore Tau halamines are likely to be generated; each of these species may act as a potential source of plasmalogen oxidation. As with the p-EA and p-Ser chloramines, the second-order rate constants for the reactions of *N*-α-acetyl-Lys and Tau chloramines were 5 orders of magnitude (i.e., 10^5-fold) slower than those for HOCl (Table 2). His side chain chloramines are also formed readily in complex systems (*17*) and are known to be highly reactive with rate constants only 5−30 times lower than those for HOCl itself (*16, 17*). This high reactivity was confirmed, with 4-imidazoleacetic acid chloramine observed to react with ethylene glycol vinyl ether only 15-fold slower than with HOCl (Table 2). Data could not be obtained for the corresponding 4-imidazoleacetic acid bromamine due to the instability of this species. Other bromamines did however react with ethylene glycol vinyl ether, with *N*-α-acetyl-Lys and Tau bromamines reacting somewhat more slowly than the p-EA and p-Ser bromamines; these values are only 900- and 2700-fold lower than the rate constants for HOBr (Table 2). These bromamines, the His side chain chloramines, and possibly the Lys-derived chloramines are therefore potential sources of plasmalogen oxidation in complex systems.

In addition to undergoing halogen transfer reactions, halamines can also decompose via radical pathways (*33*). Evidence has been presented for the induction of lipid peroxidation in low-density lipoproteins treated with HOCl, by chloramine-derived radicals (*34*). As the vinyl ether linkage of plasmalogens is susceptible to radical damage (reviewed in ref *9*), it is possible that *N*-centered radicals formed from chloramines (or bromamines) (*33, 35*) may provide an alternative pathway for HOX and halamine-mediated plasmalogen damage. Similar reactions have been observed recently with non-plasmalogen phospholipids (*36*); the higher reactivity of vinyl ethers over isolated double bonds makes these reactions likely. It should be noted, however, that these radical pathways would not yield the α-chloro and α-bromo fatty aldehydes that have been detected in vivo (*11, 12, 28*).

The chloramine data reported here are consistent with the general trend that primary chloramines exhibit a 10^3- to 10^6-fold decrease in reactivity compared with HOCl with a wide range of biological substrates (*6, 16, 24, 37*). Previous data on the reactions of chloramines with thiols have shown that their rate constants decrease in the order histamine > *N*-α-acetyl-Lys > Gly > Tau (*37, 38*). Although the overall reactivity of the vinyl ether moiety observed here with chloramines is much less than that for thiols, the *order* of reactivity is similar, p-Ser > p-EA ∼ *N*-α-acetyl-Lys > Tau, except the α-amino chloramine of p-Ser is relatively more reactive than the α-amino chloramine of Gly; the reason for the latter difference remains to be established. Similar comparisons for bromamines are not possible as yet, as few rate constants for bromamine reactions are available (reviewed in ref *6*). However, the data presented here suggest that the oxidizing capacity of HOBr is attenuated far less by its conversion to bromamines than the corresponding conversion of HOCl to chloramines.

Several studies have indicated that plasmalogens are depleted in a number of human pathologies, including Alzheimer's disease, Down syndrome, multiple sclerosis, hypercholesterolemia and ischemia-reperfusion injury, as well as in aging (*9, 26, 39*). This depletion of plasmalogens may result from oxidative damage, peroxisomal disorders that impair plasmalogen biosynthesis, or stimulation of receptor-mediated degradative enzymes such as plasmalogen-specific phospholipase A_2 (*9, 39*). In people with Alzheimer's disease, a marked decrease in PE plasmalogen levels has been observed in areas of the brain that show active degeneration, and the severity of dementia correlates strongly with loss of these lipids (*39–41*). Active MPO has been detected in postmortem brain samples affected by Alzheimer's disease, and levels of the HOCl biomarker, 3-chlorotyrosine, have been shown to be elevated compared to age-matched controls (*42*). Thus, in Alzheimer's disease there is evidence for increased formation of HOCl, and decreased PE plasmalogen content; whether these observations are linked has yet to be established. In contrast, brain tissue affected by Parkinson's disease has been reported to contain elevated levels of MPO (*43*), but no decrease in PE plasmalogens (reviewed in ref *39*). Quantification of the levels of α-chloro fatty aldehydes in brain tissue from patients with Alzheimer's and Parkinson's diseases might provide insight into this potential link between inflammation, MPO and neurological diseases.

Recently studies have shown that serum plasmalogen levels correlate strongly with HDL cholesterol levels (*44*); similarly, plasmalogen levels in hypercholesterolemic patients are significantly decreased relative to normolipidemic subjects (*26*). It is well established that the risk of atherosclerosis and heart disease increases with hypercholesterolemia and

decreased HDL cholesterol levels (*45*), and there is also strong evidence that MPO and HOCl are involved in atherosclerosis (reviewed in ref *1*). Recently, it has been established that human atherosclerotic lesions contain elevated levels of unsaturated lysophosphatidylcholine (LPC) and α-chloro fatty aldehydes (*12*), major products of HOCl attack on PC plasmalogens. The average content of the latter, in human atherosclerotic lesions, was found to be ca. 1400-fold higher than in healthy aorta samples (*12*). The α-chloro fatty aldehyde, 2-chlorohexadecanal (2-ClHDA), can form Schiff base adducts with nucleophilic sites on proteins and phospholipids, and these adducts can disrupt normal protein function and membrane dynamics (*28*). 2-ClHDA also accumulates in rat hearts that have undergone myocardial infarction, and may contribute to cardiac dysfunction (*13*). LPC accumulation may also be detrimental (*46*), and result in the induction of heart arrhythmias and inhibition of membrane transport proteins (*47–49*).

HOBr and bromamines have been shown to oxidize the plasmalogen vinyl ether bond, liberating α-bromo fatty aldehydes and lysophospholipids (*11*), consistent with the kinetic data presented here. However, there are few studies to date on the role of these reactions in disease. These processes may be important in asthma and other inflammatory diseases that involve tissue infiltration by eosinophils (reviewed in ref *1*), as HOBr is one of the major oxidants generated by eosinophil peroxidase (*50*).

Overall, these studies provide definitive kinetic data on the reactions of HOCl, HOBr, chloramines and bromamines with the vinyl ether linkage of plasmalogens and confirm, and quantify, the enhanced reactivity of plasmalogens over unsaturated fatty acid side chains. These data rationalize the detection of plasmalogen, but not other unsaturated phospholipid (chlorohydrin) products, in atherosclerotic lesions and following myocardial infarction (*11, 28*). The data indicate that HOCl/HOBr-mediated plasmalogen oxidation may be important in a number of biological events, including cell lysis and lipoprotein oxidation. Furthermore, the targeting of plasmenyl-phospholipids, by myeloperoxidase and eosinophil peroxidase-derived oxidants, may be a widespread phenomenon in inflammatory diseases, and particularly in the vascular wall, in myocytes and brain tissue as these tissues are particularly rich in plasmalogens.

ACKNOWLEDGMENT

The authors thank Prof. Peter Lay and Dr. Aviva Levina (University of Sydney) for the use of the Applied Photophysics SX.18MV stopped-flow system.

REFERENCES

1. Davies, M. J., Hawkins, C. L., Pattison, D. I., and Rees, M. D. (2008) Mammalian heme peroxidases: From molecular mechanisms to health implications. *Antioxid. Redox Signaling 10*, 1199–1234.
2. Kettle, A. J., and Winterbourn, C. C. (1997) Myeloperoxidase: A key regulator of neutrophil oxidant production. *Redox Rep. 3*, 3–15.
3. Thomas, E. L. (1979) Myeloperoxidase, hydrogen peroxide, chloride antimicrobial system: Nitrogen-chlorine derivatives of bacterial components in bactericidal action against *Escherichia coli*. *Infect. Immun 23*, 522–531.
4. Thomas, E. L., Grisham, M. B., and Jefferson, M. M. (1986) Cytotoxicity of chloramines. *Methods Enzymol. 132*, 585–593.
5. Prutz, W. A., Kissner, R., Nauser, T., and Koppenol, W. H. (2001) On the oxidation of cytochrome C by hypohalous acids. *Arch. Biochem. Biophys. 389*, 110–122.
6. Pattison, D. I., and Davies, M. J. (2006) Reactions of myeloperoxidase-derived oxidants with biological substrates: Gaining chemical insight into human inflammatory diseases. *Curr. Med. Chem. 13*, 3271–3290.
7. Carr, A. C., Winterbourn, C. C., and van den Berg, J. J. M. (1996) Peroxidase-mediated bromination of unsaturated fatty acids to form bromohydrins. *Arch. Biochem. Biophys. 327*, 227–233.
8. Spickett, C. M. (2007) Chlorinated lipids and fatty acids: An emerging role in pathology. *Pharmacol. Ther. 115*, 400–409.
9. Nagan, N., and Zoeller, R. A. (2001) Plasmalogens: Biosynthesis and functions. *Prog. Lipid Res. 40*, 199–229.
10. Mangold, H. K., and Weber, N. (1987) Biosynthesis and biotransformation of ether lipids. *Lipids 22*, 789–799.
11. Albert, C. J., Thukkani, A. K., Heuertz, R. M., Slungaard, A., Hazen, S. L., and Ford, D. A. (2003) Eosinophil peroxidase-derived reactive brominating species target the vinyl ether bond of plasmalogens generating a novel chemoattractant, alpha-bromo fatty aldehyde. *Biol. Chem. 278*, 8942–8950.
12. Thukkani, A. K., McHowat, J., Hsu, F. F., Brennan, M. L., Hazen, S. L., and Ford, D. A. (2003) Identification of alpha-chloro fatty aldehydes and unsaturated lysophosphatidylcholine molecular species in human atherosclerotic lesions. *Circulation 108*, 3128–3133.
13. Thukkani, A. K., Martinson, B. D., Albert, C. J., Vogler, G. A., and Ford, D. A. (2005) Neutrophil-mediated accumulation of 2-ClHDA during myocardial infarction: 2-ClHDA-mediated myocardial injury. *Am. J. Physiol. 288*, H2955–H2964.
14. Morris, J. C. (1966) The acid ionization constant of HOCl from 5°C to 35°C. *J. Phys. Chem. 70*, 3798–3805.
15. Prutz, W. A. (1999) Consecutive halogen transfer between various functional groups induced by reaction of hypohalous acids: NADH oxidation by halogenated amide groups. *Arch. Biochem. Biophys. 371*, 107–114.
16. Pattison, D. I., Hawkins, C. L., and Davies, M. J. (2007) Hypochlorous acid-mediated protein oxidation: How important are chloramine transfer reactions and protein tertiary structure? *Biochemistry 46*, 9853–9864.
17. Pattison, D. I., and Davies, M. J. (2005) Kinetic analysis of the role of histidine chloramines in hypochlorous acid mediated protein oxidation. *Biochemistry 44*, 7378–7387.
18. Thomas, E. L., Grisham, M. B., and Jefferson, M. M. (1986) Preparation and characterization of chloramines. *Methods Enzymol. 132*, 569–585.
19. Eyer, P., Worek, F., Kiderlen, D., Sinko, G., Stuglin, A., Simeon-Rudolf, V., and Reiner, E. (2003) Molar absorption coefficients for the reduced Ellman reagent: Reassessment. *Anal. Biochem. 312*, 224–227.
20. Pattison, D. I., Hawkins, C. L., and Davies, M. J. (2003) Hypochlorous acid mediated oxidation of lipid components present in low-density lipoproteins: Absolute rate constants, product analysis and computational modeling. *Chem. Res. Toxicol. 16*, 439–449.
21. Skaff, O., Pattison, D. I., and Davies, M. J. (2007) Kinetics of hypobromous acid-mediated oxidation of lipid components and antioxidants. *Chem. Res. Toxicol. 20*, 1980–1988.
22. Pattison, D. I., and Davies, M. J. (2004) A kinetic analysis of the reactions of hypobromous acid with protein components: Implications for cellular damage and the use of 3-bromotyrosine as a marker of oxidative stress. *Biochemistry 43*, 4799–4809.
23. Pattison, D. I., and Davies, M. J. (2001) Absolute rate constants for the reaction of hypochlorous acid with protein side-chains and peptide bonds. *Chem. Res. Toxicol. 14*, 1453–1464.
24. Peskin, A. V., Midwinter, R. G., Harwood, D. T., and Winterbourn, C. C. (2004) Chlorine transfer between glycine, taurine, and histamine: Reaction rates and impact on cellular reactivity. *Free Radical Biol. Med. 37*, 1622–1630.
25. Maeba, R., and Ueta, N. (2004) Determination of choline and ethanolamine plasmalogens in human plasma by HPLC using radioactive triiodide (1-) ion ($^{125}I_3^-$). *Anal. Biochem. 331*, 169–176.
26. Brautigam, C., Engelmann, B., Reiss, D., Reinhardt, U., Thiery, J., Richter, W. O., and Brosche, T. (1996) Plasmalogen phospholipids in plasma lipoproteins of normolipidemic donors and patients with hypercholesterolemia treated by LDL apheresis. *Atherosclerosis 119*, 77–88.

27. Le*β*ig, J., Schiller, J., Arnhold, J., and Fuchs, B. (2007) Hypochlorous acid-mediated generation of glycerophosphocholine from unsaturated plasmalogen glycerophosphocholine lipids. *J. Lipid Res. 48*, 1316–1324.
28. Thukkani, A. K., Albert, C. J., Wildsmith, K. R., Messner, M. C., Martinson, B. D., Hsu, F. F., and Ford, D. A. (2003) Myeloperoxidase-derived reactive chlorinating species from human monocytes target plasmalogens in low density lipoprotein. *J. Biol. Chem. 278*, 36365–36372.
29. Spalteholz, H., Wenske, K., and Arnhold, J. (2005) Interaction of hypohalous acids and heme peroxidases with unsaturated phosphatidylcholines. *Biofactors 24*, 67–76.
30. Spalteholz, H., Panasenko, O. M., and Arnhold, J. (2006) Formation of reactive halide species by myeloperoxidase and eosinophil peroxidase. *Arch. Biochem. Biophys. 445*, 225–234.
31. Carr, A. C., van den Berg, J. J., and Winterbourn, C. C. (1998) Differential reactivities of hypochlorous and hypobromous acids with purified *Escherichia coli* phospholipid: Formation of haloamines and halohydrins. *Biochim. Biophys. Acta 1392*, 254–264.
32. Learn, D. B., Fried, V. A., and Thomas, E. L. (1990) Taurine and hypotaurine content of human-leukocytes. *J. Leukocyte Biol. 48*, 174–182.
33. Hawkins, C. L., and Davies, M. J. (1998) Hypochlorite-induced damage to proteins: Formation of nitrogen-centred radicals from lysine residues and their role in protein fragmentation. *Biochem. J. 332*, 617–625.
34. Hazell, L. J., Davies, M. J., and Stocker, R. (1999) Secondary radicals derived from chloramines of apolipoprotein B-100 contribute to HOCl-induced lipid peroxidation of low-density lipoproteins. *Biochem. J. 339*, 489–495.
35. Hawkins, C. L., and Davies, M. J. (2005) The role of reactive *N*-bromo species and radical intermediates in hypobromous acid-induced protein oxidation. *Free Radical Biol. Med. 39*, 900–912.
36. Kawai, Y., Kiyokawa, H., Kimura, Y., Kato, Y., Tsuchiya, K., and Terao, J. (2006) Hypochlorous acid-derived modification of phospholipids: Characterization of aminophospholipids as regulatory molecules for lipid peroxidation. *Biochemistry 45*, 14201–14211.
37. Peskin, A. V., and Winterbourn, C. C. (2001) Kinetics of the reactions of hypochlorous acid and amino acid chloramines with thiols, methionine, and ascorbate. *Free Radical Biol. Med. 30*, 572–579.
38. Peskin, A. V., and Winterbourn, C. C. (2003) Histamine chloramine reactivity with thiol compounds, ascorbate, and methionine and with intracellular glutathione. *Free Radical Biol. Med. 35*, 1252–1260.
39. Hartmann, T., Kuchenbecker, J., and Grimm, M. O. W. (2007) Alzheimer's disease: The lipid connection. *J. Neurochem. 103*, 159–170.
40. Goodenowe, D. B., Cook, L. L., Liu, J., Lu, Y., Jayasinghe, D. A., Ahiahonu, P. W. K., Heath, D., Yamazaki, Y., Flax, J., Krenitsky, K. F., Sparks, D. L., Lerner, A., Friedland, R. P., Kudo, T., Kamino, K., Morihara, T., Takeda, M., and Wood, P. L. (2007) Peripheral ethanolamine plasmalogen deficiency: A logical causative factor in Alzheimer's disease and dementia. *J. Lipid Res. 48*, 2485–2498.
41. Han, X. (2005) Lipid alterations in the earliest clinically recognizable stage of Alzheimer's disease: Implications in the pathogenesis of Alzheimer's disease. *Curr. Alzheimer Res. 2*, 65–77.
42. Green, P. S., Mendez, A. J., Jacob, J. S., Crowley, J. R., Growdon, W., Hyman, B. T., and Heinecke, J. W. (2004) Neuronal expression of myeloperoxidase is increased in Alzheimer's disease. *J. Neurochem. 90*, 724–733.
43. Choi, D. C., Pennathur, S., Perier, C., Tieu, K., Teismann, P., Wu, D. C., Jackson-Lewis, V., Vila, M., Vonsattel, J. P., Heinecke, J. W., and Przedborski, S. (2005) Ablation of the inflammatory enzyme myeloperoxidase mitigates features of Parkinson's disease in mice. *J. Neurosci. 25*, 6594–6600.
44. Maeba, R., Maeda, T., Kinoshita, M., Takao, K., Takenaka, H., Kusano, J., Yoshimura, N., Takeoka, Y., Yasuda, D., Okazaki, T., and Teramoto, T. (2007) Plasmalogens in human serum positively correlate with high-density lipoprotein and decrease with aging. *J. Atheroscler. Thromb. 14*, 12–18.
45. Stocker, R., and Keaney, J. F., Jr. (2004) Role of oxidative modifications in atherosclerosis. *Physiol. Rev. 84*, 1381–1478.
46. Matsumoto, T., Kobayashi, T., and Kamata, K. (2007) Role of lysophosphatidylcholine (LPC) in atherosclerosis. *Curr. Med. Chem. 14*, 3209–3220.
47. Sasaki, Y., Asaoka, Y., and Nishizuka, Y. (1993) Potentiation of diacylglycerol-induced activation of protein kinase C by lysophospholipids: Subspecies difference. *FEBS Lett. 320*, 47–51.
48. Igarashi, Y., Kitamura, K., Zhou, Q., and Hakomori, S.-i. (1990) A role of lyso-phosphatidylcholine in GM3-dependent inhibition of epidermal growth factor receptor autophosphorylation in A431 plasma membranes. *Biochem. Biophys. Res. Commun. 172*, 77–84.
49. Sedlis, S. P., Corr, P. B., Sobel, B. E., and Ahumada, G. G. (1983) Lysophosphatidyl choline potentiates Ca^{2+} accumulation in rat cardiac myocytes. *Am. J. Physiol. 244*, H32–38.
50. Weiss, S. J., Test, S. T., Eckmann, C. M., Roos, D., and Recvani, S. (1986) Brominating oxidants generated by human eosinophils. *Science 234*, 200–203.

BI800786Q